Available online at www.sciencedirect.com
ScienceDirect
Journal of Structural Biology 160 (2007) 211–223
Journal of Structural Biology
www.elsevier.com/locate/yjsbi

Spontaneous fibrillation of the native neuropeptide hormone Somatostatin-14

Wilmar van Grondelle [a], Carmen López Iglesias [b], Elisenda Coll [b], Franck Artzner [c], Maïté Paternostre [d], Frédéric Lacombe [a], Merce Cardus [a], Gema Martinez [b], Martin Montes [a], Roland Cherif-Cheikh [a], Céline Valéry [a,*]

[a] *Ipsen Pharma, Carrer Laureà Miró 395, Sant Feliu de Llobregat, 08980 Barcelona, Spain*
[b] *Unitat de Microscopía Electrónica, Serveis Cientificotecnics, Universitat de Barcelona, Spain*
[c] *Groupe Matière Condensée et Matériaux, UMR 6226, Université de Rennes I, France*
[d] *Institut de BioTechnologies de Saclay, URA 2096, CEA-Saclay, France*

Received 24 April 2007; received in revised form 6 August 2007; accepted 13 August 2007
Available online 23 August 2007

Abstract

Natural Somatostatin-14 is a small cyclic neuropeptide hormone with broad inhibitory effects on endocrine secretions. Here we show that natural Somatostatin-14 spontaneously self-assembles in water and in 150 mM NaCl into liquid crystalline nanofibrils, which follow characteristic structural features of amyloid fibrils. These non-covalent highly stable structures are based on the Somatostatin native backbone conformation and are formed under non-denaturing conditions. Our results support the hypothesis that self-assembly into amyloid fibrils is a generic property of the polypeptide chain under appropriate conditions. Given recent advances on the mechanisms of biological storage and sorting modes of peptide/protein hormones into secretory granules, we propose that Somatostatin-14 fibrillation could be relevant to the regulated secretion pathway of this neuropeptide hormone. Such a hypothesis is consistent with the emerging concept of the existence of non-disease related but functional amyloids.

Keywords: Amyloid; Somatostatin; Hormone; Self-assembly; Regulated secretion pathway

1. Introduction

Various natural peptides and proteins have been shown to self-assemble *in vitro* into amyloid-like β-sheet rich supramolecular fibrils. Typical amyloid fibrils, exhibit a diameter of 7–12 nm, are constructed with twisted protofilaments and are further integrated to form higher order association fibers. Their inner supramolecular structure relies on β-sheet hydrogen bonds networks developed along the fibril director, the so-called "cross-β" organization (Serpell, 2000; Sunde et al., 1997). The variety of sequences able to form amyloid-like fibrils raised the idea of a generic feature coming from intrinsic properties of polypeptide chains under appropriate conditions (Chiti et al., 1999; Dobson, 1999). However, the physiological significance of such self-assemblies is generally not fully understood or often associated to disease-related misfolding. In fact most of the fibrillar aggregates of natural peptides and proteins are observed under denaturing conditions, such as extreme conditions of pH, temperature or ionic strength. In this context, a few natural peptide and protein hormones were shown to form fibrillar self-assemblies based on disease-related misfolding under denaturing conditions, such as insulin (Krebs et al., 2004; Waugh, 1946), calcitonin (Haspel et al., 2005; Reches et al., 2002) and amylin (Kajava et al., 2005; Tracz et al., 2004). Meanwhile, non-disease related aggregates were evidenced *in vivo* for a few natural peptide and protein hormones, such as prolactin, growth hormone, chromogranins, or insulin, close to or within their storage

* Corresponding author. Fax: +34 936851011.
E-mail address: celine.valery@ipsen.com (C. Valéry).

1047-8477/$ - see front matter © 2007 Elsevier Inc. All rights reserved.
doi:10.1016/j.jsb.2007.08.006

site. These findings led to the hypothesis that biological storage of some hormones could rely on reversible aggregation mechanisms (Arvan, 1998; Dannies, 1999). Recent investigations further suggested the involvement in these mechanisms of self-organized aggregates based on native hormone conformations (Keeler et al., 2004). Given the latter hypothesis, structural *in vitro* investigation of the self-assembling propensities of natural hormones under non-denaturing conditions can give insights such aggregation mechanisms. This was attempted for a few protein hormones, but the size of the molecules studied, more particularly their high potential to adopt various conformations and so, to be denatured *in vitro*, made these investigations difficult to correlate with *in vivo* observations (Dannies, 1999). Small and conformationally constrained natural peptide hormones are relatively better suited systems to investigate these propensities *in vitro* under relevant conditions, since their conformational freedom is limited and so is their misfolding propensity.

Natural Somatostatin-14 is a small cyclic neuropeptide hormone that is unique in its broad inhibitory effects on endocrine secretions. It was not only shown to regulate growth hormone (Brazeau et al., 1973), glucagon, insulin (Mandarino et al., 1981) and gastrin secretions (Bloom et al., 1974), but also to modulate cognitive processes (Schettini, 1991). For Somatostatin-14 at low concentrations in water, as well as in other solvents, earlier works showed a high propensity for antiparallel β-sheet and β-turn secondary structures. A model conformation in solution based on a β-hairpin has been proposed and further related to the Somatostatin biological activity (Holladay and Puett, 1976; Holladay et al., 1977). Since then, the design of potent Somatostatin therapeutic analogs has put the emphasis on the stabilization of the β-turn (Reisine and Bell, 1995; Veber et al., 1978; Weckbecker et al., 2003). One of such Somatostatin analogs, the synthetic octapeptide Lanreotide, has been recently shown to spontaneously self-associate in water into original liquid crystalline nanotubes with four hierarchical levels (Valéry et al., 2003, 2004). The Lanreotide nanotubes were shown to be based on a fixed β-hairpin conformation developing intermolecular antiparallel β-sheet networks, and on an original aromatic/aliphatic residues segregation that is kept in the different inner hierarchical levels. The sequence analogy between Lanreotide and Somatostatin suggests that the natural neuropeptide hormone could have the propensity to self-assemble into supramolecular structures under native conditions.

Here we report the investigation of the spontaneous self-assembling properties of natural Somatostatin-14 (as acetate salt) under non-destabilizing conditions in aqueous media. To get insight into the structure of the self-assemblies at both supramolecular and molecular scales, the investigation was conducted by using complementary physicochemical techniques, including optical and electron microcopy (negative staining and freeze-fracture/etching), X-ray scattering, size-exclusion and reverse-phase HPLC, and vibrational spectroscopy (ATR-FTIR).

2. Material and methods

2.1. Material

Somatostatin-14 (Ala-Gly-Cys-Lys-Asn-Phe-Phe-Trp-Lys-Thr-Phe-Thr-Ser-Cys, MW 1638 Da) was purchased from Lipotec (Gava, Spain). A drawing of the peptide is provided as Supplementary material 1. The peptide was obtained as an acetate salt, with content in acetate of 8.3%w/w. Congo Red staining solution was obtained from Sigma (Spain). Uranyl acetate was obtained from Merck (Darmstadt, Germany) and sodium chloride 0.9%w/w (150 mM) in water was obtained from Braun (Spain). Fresh purified water obtained from a Millipore filtration system was used for samples preparation.

2.2. Samples preparation

Water or NaCl 150 mM in water was added to a weighed fraction of Somatostatin-14 acetate powder. Mixing was realized using a vortex for a few seconds to one minute. Samples were stored at 4 °C and allowed to reach room temperature (25 °C) for at least one hour before performing experiments. The pH of the Somatostatin acetate solutions was measured just after dissolution of Somatostatin acetate in the aqueous media, i.e., before formation of the anisotropic phases. It was found to remain around pH 4.7 ± 0.3 in the range of concentrations studied. Under these conditions, the peptide exhibits a net charge of +2 (calculated p*I* of 8.3).

2.3. Optical microscopy and Congo Red birefringence assays

Optical microscopy observations were performed using an Axiovert 100A Olympus inverted microscope, at magnifications up to 20× (A-plan Olympus objectives), on samples conditioned in thin layers between glass coverslips. The polarizer and analyzer were in a fixed crossed position. A λ-retardation plate was inserted at 45° to the polarizers. Experiments were either performed at room temperature (25 °C) or while applying temperature gradients, by using a homemade Pelletier heating plate adapted to the microscope, and controlled via a computer. For such temperature-dependent experiments, observations were made every 5–10 °C from 25 to 80 °C, after having let the sample reach the chosen temperature during 5–10 min (until no observed evolution). Digital images were taken with an Olympus Highlight 3000 camera connected to a computer.

Congo Red birefringence assays were performed as described by Nilsson (2004), by air-drying 10 μL of peptide solutions onto glass coverslips and by placing around 200 μL of Congo Red staining solution onto the dried peptide samples. After a few seconds, the excess solution was removed with hardened filter paper without touching the sample. After allowing the stained samples to dry at room temperature, the stained domains were first localized with optical microscopy in the bright field configuration, by

detection of the characteristic deep red color of the dye. Polarized light optical microscopy was then used in these domains to search for the green/yellow birefringence characteristic of Congo Red binding to amyloid-like peptide/protein assemblies.

2.4. Reverse-phase HPLC (RP-HPLC)

The Waters HPLC system consisted of two W515 pumps, a W717 Autosampler and a W486 UV detector. Chromatography was performed on a Waters Symmetry C_{18} column (5 μm particle size, 150 × 3.9 mm). Experiments and acquisition were controlled using the Waters Empower C/S software. Trifluoracetic acid (TFA) 0.1% v/v in water was used as mobile phase and acetonitrile in water 60/40 v/v with 0.1% v/v TFA was used as organic eluent. The Somatostatin-14 acetate aqueous samples were diluted in water/acetic acid 0.1% v/v to reach peptide concentrations around 0.5 mg/mL. Twenty microliters (around 10 μg peptide) of the diluted solutions was injected. Separation was carried out at room temperature, at a flow rate of 1 mL/min, with a gradient from 30% to 60% of organic eluent in the mobile phase in 60 min. Detection was performed at 215 nm. The retention time of Somatostatin-14 under these conditions was approximately 35 min. Freshly prepared solutions of Somatostatin-14 acetate in water/acetic acid 0.1% v/v and of known peptide concentration (around 0.5 mg/mL) were used to generate calibration curves (standard solutions).

2.5. Size-exclusion HPLC (SEC-HPLC)

The Waters HPLC system consisted of a W600 pump, a W717 autosampler and a 996 Photo Diode Array detector. Chromatography was performed on a Tosoh Bioscience TSK G3000 SW XL column (7.8 × 300 mm). Experiments and acquisition were controlled using the Waters Empower C/S software. Acetonitrile in water (30/70 v/v) with 0.05% v/v TFA was used as mobile phase. The Somatostatin-14 acetate aqueous samples were diluted in water/acetic acid 0.1% v/v to reach peptide concentrations around 0.5 mg/mL. Twenty microliters (around 10 μg peptide) of the diluted solutions was injected. Isocratic separation was performed at 30 °C at a flow rate of 0.6 mL/min. The column eluent was analyzed in the range 200–400 nm. The retention time of Somatostatin-14 under these conditions was approximately 15 min. Freshly prepared solutions of Somatostatin-14 acetate in water/acetic acid 0.1% v/v and of known peptide concentration (around 0.5 mg/mL) were used to generate calibration curves (standard solutions).

2.6. Negative staining

Carbon-coated Formvar 200-mesh copper grids were deposited successively for one minute each onto 15 μL drops of (i) Somatostatin-14 acetate aqueous solutions, (ii) water (3 times) and (iii) 0.2%w/w uranyl acetate in water. Paper filter was used to remove the excess liquid from the grids, which were then let to dry for one day before electron microscopy observations.

2.7. Freeze-fracture and freeze-etching (FFEM)

Drops of Somatostatin-14 acetate solutions were sandwiched between two copper platelets using a 400-mesh gold grid as spacer. The samples were then frozen at −190 °C by rapid immersion in liquid propane and stored at −196 °C in liquid nitrogen until subsequent use. Frozen samples were fractured at −150 °C and 2×10^{-8} mbar in a Baltec BAF 060 freeze-fracture apparatus (BAL-TEC, Liechtenstein). Freeze-etching was carried out by switching the sample temperature from −150 to −100 °C and maintaining the pressure at 10^{-7} mbar for 2 min to sublimate the surface layer of ice. Metal replicas of the exposed surfaces were obtained by evaporating 2 nm of platinum with an electron gun at an angle of 45° and 20 nm of carbon with an electron gun at an angle of 90°. After being floated in distilled water, the replicas were picked up on Formvar-coated EM grids.

2.8. Transmission electron microscopy (TEM)

Either stained samples or freeze-fracture replicas, which were previously deposited on 200-mesh Formvar-coated copper grids, were examined with a JEOL 1010 transmission electron microscope at 80 kV.

2.9. Attenuated total reflectance Fourier-transform infrared spectroscopy (ATR-FTIR)

Attenuated total reflectance FTIR spectra were measured at 4 cm^{-1} resolution using a Bruker (Billerica, MA) IFS 66 spectrophotometer equipped with a 458 n ZnSe ATR attachment. The spectra shown resulted from the average of 30 scans. All spectra were baseline corrected and the water signal was removed by subtraction of the pure water spectrum recorded the day of experiment. For all the spectra, the area between 1600 and 1700 cm^{-1} was normalized to unity. Analysis of Somatostatin-14 conformation was performed by deconvolution of the absorption spectra, either as a sum of Gaussian components (Susi and Byler, 1986) or as a sum of spectra assigned to different structures (Venyaminov and Kalnin, 1990).

2.10. Wide angle X-ray scattering (WAXS)

X-ray patterns were collected with a Mar345 Image-Plate detector (Maresearch, Norderstedt, Germany) mounted on a rotating anode X-ray generator FR591 (Bruker, Courtaboeuf, France) operated at 50 kV and 50 mA. The monochromatic CuKα radiation ($\lambda = 1.541$ Å) was focalized with a 350 μm focal spot at 320 mm by a double reflection on a elliptic cross multi-layer Montel mirror (Incoatec, Geesthacht, Germany). The beam was defined

under vacuum by four motorized carbon–tungsten slits (JJ-Xray, Roskilde, Denmark) positioned in front of the mirror (500 μm). Four additional guard slits were placed at the focal point with a 220 mm slit separation distance. The flux after the output mica windows was 3×10^8 photons/s. A 2 mm diameter circular lead beam stop was placed in air at 150 mm afterward the sample and the detector was positioned at 360 mm. The X-ray patterns were therefore recorded for a range of reciprocal spacing $q = 4\pi^* \sin\theta/\lambda$ from is 0.03–1.8 Å^{-1} where θ is the diffraction angle. The repetition distances $d = 2\pi/q$ should be between 200 Å and 3.5 Å. The samples were placed into 1.2–1.3 mm glass capillaries (Glas W.Müller, Germany) and introduced into a homemade capillaries holder, which can maintain up to 20 capillaries at a controlled temperature.

3. Results

3.1. Spontaneous lyotropic behavior and Congo Red binding

Birefringence was characterized to occur at room temperature from around 3%w/w (30 mg/mL) of Somatostatin acetate in water, with a significant lag time of a few hours to a few days. At macroscopic scale, birefringence occurrence was correlated to turbidity and viscosity increase. A similar behavior was observed in the presence of NaCl 150 mM, however from around 0.5%w/w of Somatostatin acetate. Somatostatin-14 therefore spontaneously forms anisotropic phases in both aqueous media. The shift of the limit concentration of formation towards lower values in the presence of 150 mM NaCl supports the idea that this process is favored by ionic strength increase.

Optical textures were obtained between 3% and 20%w/w of peptide acetate in water, in particular developable domains-like textures together with threaded textures, without any specificity to peptide concentration (Fig. 1A). Observations using a retardation plate confirmed these patterns to be due to specific liquid crystalline defects, which arise from continuous orientation variations of the slow (blue) and fast (orange) optical axes of the birefringent objects (Fig. 1B). Similar textures were formed in the presence of NaCl 150 mM, between 0.5% and 10%w/w of Somatostatin acetate (Fig. 1C and D). The threaded textures in 150 mM NaCl were observed to reach widths up to about 130 μm versus 50 μm for the ones in pure water (Fig. 1A and D). Developable domains result from the curvature of objects that globally remain parallel one to another, i.e., are either due to columnar or lamellar phases (Bouligand, 1998). Threaded textures result from local and periodic variations in molecular orientation, and generally arise from nematic phases (Viney and Putnam, 1995). Somatostatin-14 therefore spontaneously self-organizes at room temperature into columnar or lamellar liquid crystalline phases with nematic properties, in pure water and in 150 mM NaCl, within a wide range of peptide acetate concentrations. However, according to the literature, the width

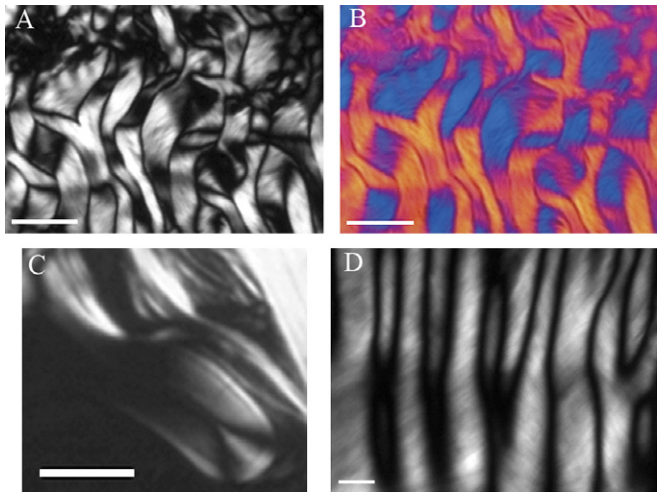

Fig. 1. Optical textures under crossed polarizers (A, C and D) and with an additional retardation plate (λ) (B). Developable domain-like textures combined to threaded textures, obtained for Somatostatin-14 acetate 15%w/w in water (A and B). Developable-like texture (C) and threaded textures (D) obtained for Somatostatin-14 acetate 5%w/w in 150 mM NaCl in water. Scale bars 100 μm.

increase for the threaded textures in 150 mM NaCl indicates an enhanced orientational freedom of the corresponding liquid crystals, relatively to the ones in pure water (Viney and Putnam, 1995).

Congo Red birefringence assays were performed on the Somatostatin-14 mesophases formed in both pure water and in 150 mM NaCl (Fig. 2), as a common optical test indicative of the presence of amyloid-like assemblies (Nilsson, 2004). In the zones stained with Congo Red that were localized under bright field (Fig. 2A), yellow/green birefrin-

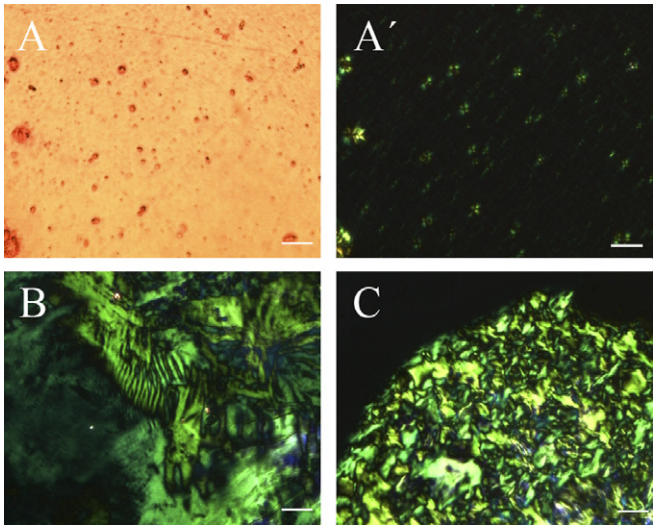

Fig. 2. Congo Red birefringence assays on self-assembled peptide samples. Bright field observation (A) and polarized light observation (A′) of Somatostatin-14 acetate 3%w/w in water stained with Congo Red. Polarized light observations of stained Somatostatin-14 acetate 15%w/w in water (B) and Somatostatin-14 acetate 10%w/w in 150 mM NaCl (C). Scale bars 100 μm except (B) 50 μm.

gence could be observed under polarized light (Figs. 2A–C). This result reveals that the columnar/lamellar liquid crystals formed by Somatostatin-14 bind the dye Congo Red, like amyloid fibrils. The corresponding Somatostatin-14 self-assemblies are therefore likely to exhibit some similar structural features to amyloid fibrils.

3.2. Mesophase and peptide stability

The chemical stability of Somatostatin-14 was previously investigated in isotropic aqueous solutions by HPLC procedures (Herrmann and Bodmeier, 2003). Here, the chemical stability of Somatostatin-14 (acetate) within its aqueous mesophases was investigated by both reverse-phase (RP) and size-exclusion (SEC) HPLC on samples kept over one month (40 days) at 37 °C. Prior to these experiments, the thermotropism of the Somatostatin-14 mesophases was assessed by temperature-dependent polarized light microscopy and by differential scanning calorimetry (DSC). The mesophases were not observed to undergo any transition up to at least 80 °C, even around the limit concentrations of mesophase formation, both in water and in 150 mM NaCl, and even when applying fast heating/cooling rates in the DSC experiments (10 °C/min, data not shown). The Somatostatin-14 mesophases are therefore highly thermally stable.

SEC- and RP-HPLC were performed for Somatostatin-14 samples in the range 0.05–20%w/w of peptide acetate in water and 1–10%w/w in NaCl 150 mM. The results obtained after storage at 37 °C during 40 days (t_{40}) were compared to the ones obtained for the same samples freshly prepared (t_0), i.e., before or while formation of the mesophases for concentrations over the limits of mesophase formation (Table 1). In all the recorded chromatograms, Somatostatin-14 gave rise to a sharp and reproducible peak. All the corresponding retention times were similar to the ones obtained for the freshly prepared standard Somatostatin-14 solutions. At t_0 all the peptide purity values were found over 98%Ar by RP-HPLC and all the monomer contents over 99%Ar by SEC-HPLC. At t_{40} all the samples in water exhibited peptide purity values over 96–97%Ar by RP-HPLC and monomer contents over 98%Ar by SEC-HPLC. The samples with 150 mM NaCl then exhibited peptide purity values over 98%Ar by RP-HPLC and monomer contents over 99%Ar by SEC-HPLC.

Table 1
RP- and SEC-HPLC results

Somatostatin-14 acetate aqueous samples kept at 37 °C	RP-HPLC Peptide purity (%Ar)		SEC-HPLC Monomer (%Ar)	
	t_0	t_{40}	t_0	t_{40}
Fresh standard solution	97.7	98.7	99.4	99.5
0.05%w/w in water	98.2	96.1	99.8	99.2
0.1%w/w in water	98.5	97.4	99.6	99.5
15%w/w in water	98.4	97.2	99.5	98.2
20%w/w in water	98.5	97.2	99.5	98.5
1%w/w in NaCl/water	98.8	98.6	99.5	99.4
3%w/w in NaCl/water	98.7	98.5	99.4	99.2
10%w/w in NaCl/water	98.8	98.7	99.5	99.3

Therefore no significant covalent aggregation could be detected in the Somatostatin-14 samples. In addition, the results did not show any significant correlation between chemical degradation and Somatostatin-14 acetate concentration. They nevertheless suggest a slightly enhanced chemical stability in the presence of NaCl. It can be concluded that the spontaneous formation of Somatostatin-14 mesophases does not alter the chemical stability of the peptide, relatively to the corresponding isotropic solutions. It further confirms that the mesophases are only due to non-covalent bonds. The fact that the Somatostatin-14 mesophases were found to be stable up to at least 80 °C reveals a strong set of non-covalent intermolecular interactions/forces involved in their structure.

3.3. Characteristic morphology of the self-assemblies

The morphology of the Somatostatin-14 self-assemblies within the aqueous mesophases was investigated by TEM on negatively stained samples. The electron micrographs obtained for 3%w/w of Somatostatin-14 acetate in water evidenced the formation of at least 8 μm long nanofibrils (Fig. 3A). The observation of nanofibrils flexibility and tendency to locally laterally align is consistent with the columnar and nematic optical textures previously obtained. Statistics performed on the nanofibrils widths showed a Gaussian distribution centered on 10–11 nm (Fig. 3D, gray plot). Smaller scale observations evidenced a twisted periodic feature in the Somatostatin-14 nanofibrils structure, which strongly suggests twisted fibrillar substructures (Fig. 3B and zoom herein). For 1%w/w of Somatostatin acetate in the presence of 150 mM NaCl, similar flexible nanofibrils were observed, also at least 8 μm long (Fig. 3C). Like in water, a twisted structural feature could be further distinguished in the larger nanofibrils, suggesting fibrillar substructures (zoom in Fig. 3C). The distribution of the nanofibrils widths, centered on around 7 nm, was found slightly smaller than in pure water (Fig. 3D, white plot).

The Somatostatin-14 self-assemblies observed in water and in 150 mM NaCl are therefore flexible liquid crystalline nanofibrils, which exhibit comparable morphologies and sizes to typical amyloid fibrils. In both media, the observations suggested subfibrillar structures that resemble the protofilament substructures of amyloid fibrils (Serpell, 2000). The presence of 150 mM NaCl was found to influence this morphology towards slightly smaller widths. In fact, the effect of NaCl on the nanofibril width was found to be significant from around 100 mM NaCl at the peptide concentrations studied (Supplementary material 2, panels A–C). This slight structural variation relatively to the nanofibrils in pure water could be one of the origins of the enhanced orientational freedom previously suggested by polarized light microscopy.

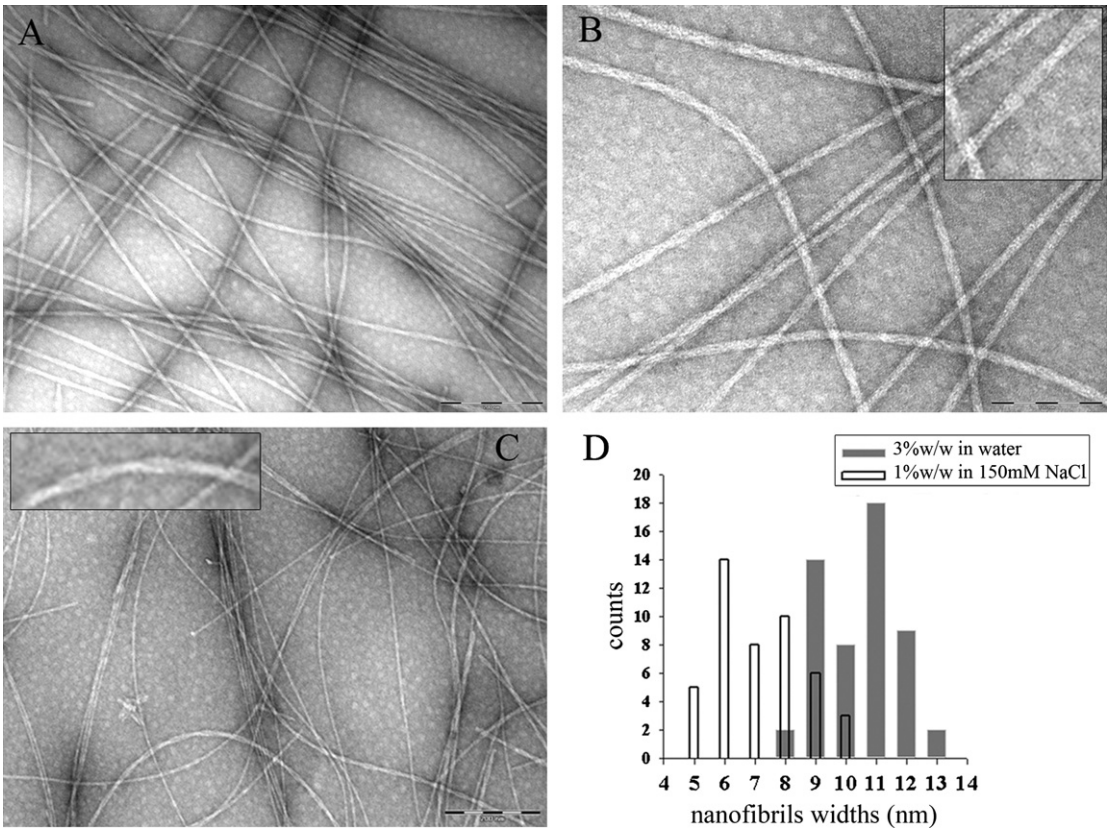

Fig. 3. Electron micrographs after negative staining (A, B and C) and corresponding measurements (D). (A) Somatostatin-14 acetate 3%w/w in water. Scale bar 200 nm. (B) Somatostatin-14 acetate 3%w/w in water. Scale bar 100 nm. (C) Somatostatin-14 acetate 1%w/w in 150 mM NaCl/water. Scale bar 200 nm.

3.4. Nanofibrils lateral association

The morphology of the Somatostatin-14 liquid crystalline structures formed at relatively high concentrations of peptide acetate was investigated by FFEM (Fig. 4). The electron micrographs obtained for 15%w/w of Somatostatin-14 acetate in water evidenced long twisted fibrillar structures. Two main morphologies could be distinguished. On one side twisted and flexible nanofibrils, at least 10 μm long and around 10–11 nm wide, were observed to exhibit a high tendency to laterally align (Fig. 4A and B). These structures are similar to the amyloid-like nanofibrils previously evidenced at lower concentration. On the other side, nanofibers mainly resulting from the close association of two twisted 10–11 nm nanofibrils were observed. Interestingly the width of these nanofibers is about twice the width of individual nanofibrils, as shown on the corresponding measurements histogram (Fig. 4C). This histogram points out this coexistence of nanofibers, i.e., associated nanofibrils, and individual nanofibrils. The nanofibrils intertwists always showed to be left-handed and to tend to occur with a regular period, mainly about twice the value of the nanofibers widths. Some amyloid fibrils have been reported to be able to further integrate into higher order fibers (Serpell, 2000). In addition, the amyloid fibrils for which the twist orientation has been determined, have been reported to exhibit a left-handed helical twist (Jimenez et al., 2002). The Somatostatin-14 structures in water therefore follow these previously reported features. The fact that the intertwists tend to regularly occur could be an indication of a structural constraint due to specific inter-nanofibrils interactions.

The electron micrographs obtained for the mesophase at 10%w/w of Somatostatin-14 acetate in the presence of 150 mM NaCl showed two main patterns. On one side, laterally tightly aligned nanofibrils with widths comprised between 5 and 11 nm were observed, i.e., similarly to the observed amyloid-like nanofibrils at lower peptide concentration in NaCl (Fig. 5A). On the other side, about twice wider and very flexible nanofibers that further exhibited a high twist periodicity were observed (Fig. 5B). However, the left-handed specificity previously observed in water was here lost. Given the previous observation in water of intertwisted nanofibrils, the twisted fibrillar patterns in the presence of 150 mM NaCl are assigned to closely intertwisted nanofibrils into higher order nanofibers. This interpretation suggests that the presence of NaCl enhances the intertwisting tendency. Given that the peptide is highly charged under the conditions used (net charge of +2, calculated p*I* of 8.3), the enhancement of nanofibril lateral association in the presence of NaCl could be due to electrostatic shielding. The direct influence of ionic strength on the lat-

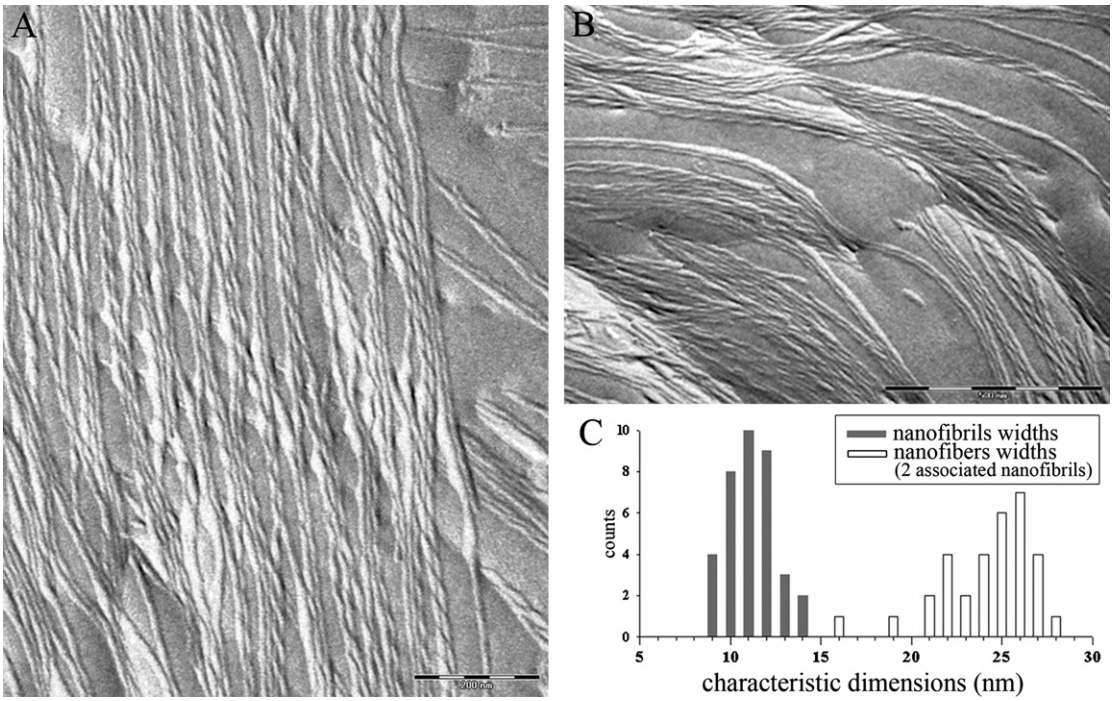

Fig. 4. Electron micrographs (A and B) of freeze-fracture/freeze-etching replicas of Somatostatin-14 acetate 15%w/w in water, scale bars 200 nm, and corresponding measurements (C).

eral association of nanofibrils was confirmed by the effect of multivalent ions (calcium and phosphate) that both increased this tendency (Supplementary material 2, panels D–F). Indeed, for both multivalent ions, bundles of closely laterally associated nanofibrils were observed for significantly lower peptide concentrations than above. In addition, the influence towards smaller nanofibril mean widths was also confirmed.

The above observations support that both peptide concentration and ionic strength promote the lateral association of the Somatostatin-14 nanofibrils. Given the formation in both water and 150 mM NaCl of higher order nanofibers, three hierarchical levels of fibrillar self-association are therefore now suggested: subfibrillar structures, nanofibrils and nanofibers. This hierarchy highly resembles the amyloid hierarchy from protofilaments to fibrils into fibers (Serpell, 2000).

3.5. Nanofibrils inner symmetries

The symmetries of the nanofibrils were further investigated by wide angle X-ray scattering. A slightly aligned X-ray pattern was obtained for 10%w/w of Somatostatin-14 acetate in 150 mM NaCl (Fig. 6A and B). This X-ray pattern exhibits 4.8 Å ($q = 1.3$ Å^{-1}) reflections aligned on the meridional axis, together with smaller angle diffuse scattering on the equatorial axis. This anisotropic combination resembles typical amyloid-like "cross-β" fiber diffraction pattern (Serpell, 2000; Sunde et al., 1997). The meridional reflections at 4.8 Å ($q = 1.3$ Å^{-1}) typically arise from the spacing along the nanofibril axis between adjacent

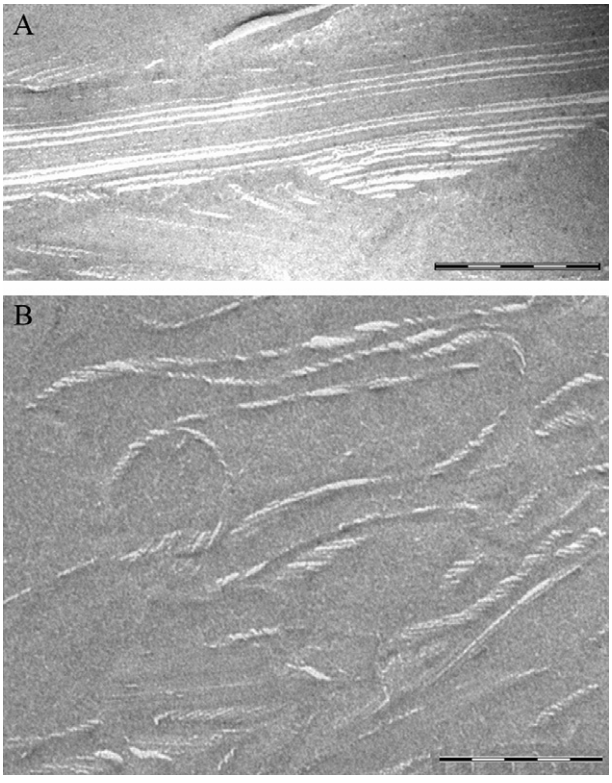

Fig. 5. Electron micrographs (A and B) after freeze-fracture/freeze-etching of mesophases of Somatostatin-14 acetate 10%w/w in 150 mM NaCl/water, scale bars 200 nm.

hydrogen-bonded β-strands. Broad equatorial diffuse scattering at small angles arises from the anisotropic form fac-

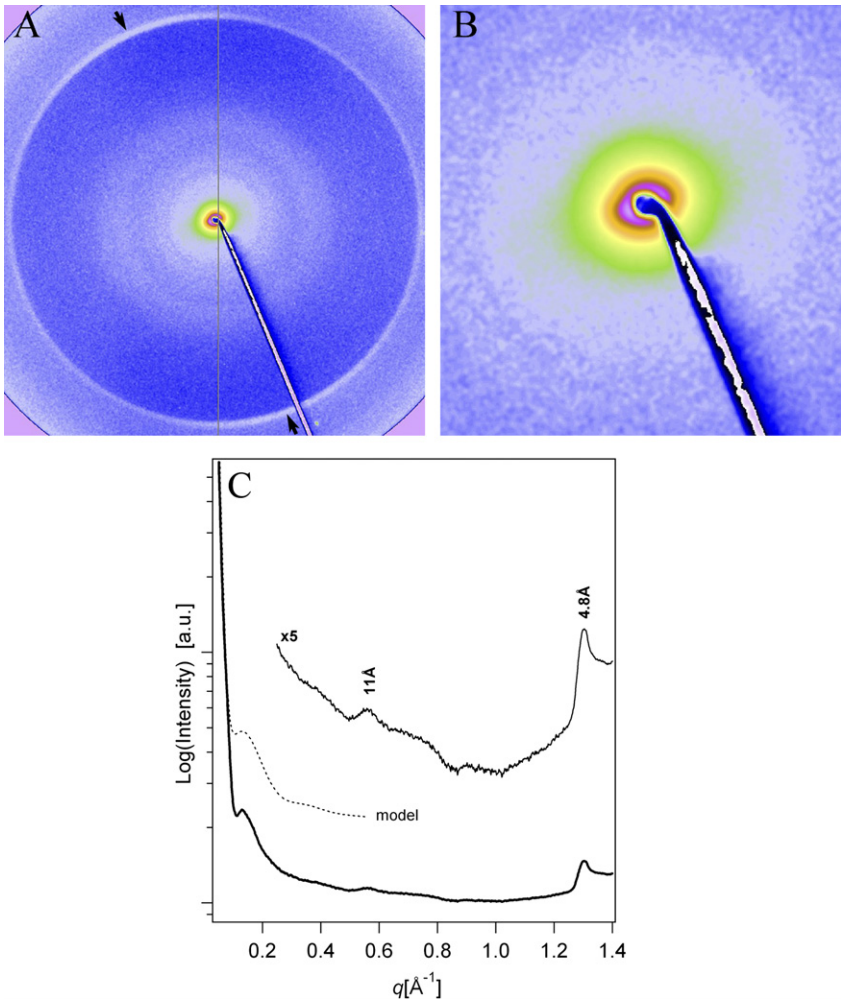

Fig. 6. X-ray scattering. (A) slightly oriented WAXS pattern recorded for Somatostatin-14 acetate 10%w/w in 150 mM NaCl in water. The meridian peak (arrows) is detected at 1.3 $Å^{-1}$ (4.8 Å); (B) zoom (4×) on the corresponding oriented equatorial patterns which are elongated perpendicularly to the fibril axis. (C) Integration profile of a non-oriented WAXS pattern recorded for Somatostatin-14 acetate 15%w/w in water and zoom on the corresponding WAXS profile; dotted line : small angle scattering model of individual layer with a thickness of 33 Å (see text).

tor of the nanofibrils and is perpendicular to the nanofibril axis (Guinier, 1994). Although no oriented X-ray pattern could be obtained for the Somatostatin-14 mesophases in water, the powder pattern corresponding to the radial profile is here showed for 15%w/w of peptide acetate in water (Fig. 6C). The same reflection at 4.8 Å was recorded indicating the amyloid-like "cross-β" organization. Additionally, a broad diffuse scattering is detected at 11 Å and should be attributed to the lateral distance between two peptide backbones in the nanofibrils, likely the intersheet stacking Valéry et al. (in press). The small angle diffuse scattering exhibits two successive maxima, and could be well fitted with a simple model of scattered intensities $I(q) = A{\cdot}(\cos(q{\cdot}e/2)/q^2)^2$, where $e = 33$ Å is the thickness of a layer (Guinier, 1994). This indicates a layered organization as observed with some Somatostatin analogs Valéry et al. (in press). The small angle X-ray diffuse scattering does not originate from the packing of nanofibrils. The X-ray data therefore show that the Somatostatin-14 nanofibrils exhibit generic structural features of amyloid fibrils, at the level of peptide intermolecular networks. This is consistent with the single nanofibrils amyloid-like morphology and sizes that were previously observed by TEM in both pure water and in the presence of 150 mM NaCl.

3.6. Backbone conformation

The conformation of the Somatostatin-14 backbone was investigated by ATR-FTIR spectroscopy. The analysis was focused on amide I vibrations (1600–1700 cm^{-1}), which mainly arise from vibrational stretching modes of the backbone carbonyl groups. According to the literature, the corresponding wavenumbers can be assigned to different strengths/types of hydrogen bonds, in which the backbone carbonyl groups are involved. They can therefore indicate secondary structure types (Hiramatsu and Kitagawa, 2005; Krimm and Bandekar, 1986). The ATR-FTIR spectra were recorded for the Somatostatin-14 mesophases in both pure water and 150 mM NaCl (Fig. 7). From 3% to 20%w/w of Somatostatin acetate in water, the amide I

vibrations exhibited an evolution directly correlated to concentration (Fig. 7A). From an unstructured amide I centered around 1645 cm^{-1} for 3%w/w, the spectra evolved towards well-defined vibrations for 20%w/w. The structured amide I could be fitted from 5%w/w by four vibrations around 1615, 1643, 1663 and 1675 cm^{-1} respectively, with an additional fifth vibration around 1627 cm^{-1} arising from 10%w/w and well-defined for 20%w/w. For the Somatostatin-14 mesophases in 150 mM NaCl, the spectra exhibited structured amide I from 3%w/w (Fig. 7B). From this concentration, the spectra could be fitted by the same five well-defined vibrations that were detected from 10%w/w in water. The fact that the amide I becomes structured for the Somatostatin mesophases supports a correlation between these well-defined vibrations and the peptide self-assemblies. Thanks to the significant lag phase of mesophase formation, it could be confirmed for a same 15%w/w peptide acetate solution in water that the evolution from unstructured to structured amide I vibrations was correlated to the formation of a mesophase and thus nanofibrils occurrence (Supplementary material 3). It confirms that the rising of these vibrations is not intrinsic to the peptide in solution, even at high concentrations, but is directly due to the Somatostatin supramolecular nanofibrils. The fact that structured amide I vibrations are recorded show that the Somatostatin-14 backbone adopts a fixed and well-defined conformation in the mesophases in both media. In accordance with the literature, the vibration around 1643 cm^{-1} is assigned to random conformations, the combination of vibrations around 1615 and 1675 cm^{-1} to antiparallel β-sheet secondary structure, and the vibration around 1663 cm^{-1} to a turn secondary structure. This combination is typical of a β-hairpin backbone conformation, which corresponds to the bioactive Somatostatin-14 conformation (Holladay and Puett, 1976; Holladay et al., 1977). The fact that strong vibrations were recorded for antiparallel β-sheet hydrogen bonds in both media indicates the development of intermolecular antiparallel β-sheet networks from the β-hairpin strands. This result is consistent with the cross-β organization previously revealed by X-ray scattering, which is characteristic of amyloid structures. The additional vibration around 1627 cm^{-1} detected from 10%w/w of Somatostatin acetate in water and from 3%w/w in NaCl 150 mM occurs in the range of wavenumbers generally assigned to β-sheet hydrogen bonds. However for most amyloid-like systems, only one strong vibration is recorded in this range of wavenumbers (Bouchard et al., 2000; Hamodrakas et al., 2004). For Somatostatin in aqueous media two vibrations are recorded in this range, at 1615 and 1627 cm^{-1}. A similar couple of vibrations was recorded in this range for fibril forming peptides from the binding region of the tau protein (Goux et al., 2004). It was then assigned to different β-sheet networks arising from multiple aggregation states. In the case of Somatostatin, the previous electron microscopy observations indicate that the occurrence of the 1627 cm^{-1} vibration does not correlate to nanofibril formation but could be linked to the lateral association of these into nanofibers. The rising of this vibration could therefore be directly or indirectly due to specific inter-nanofibril interactions.

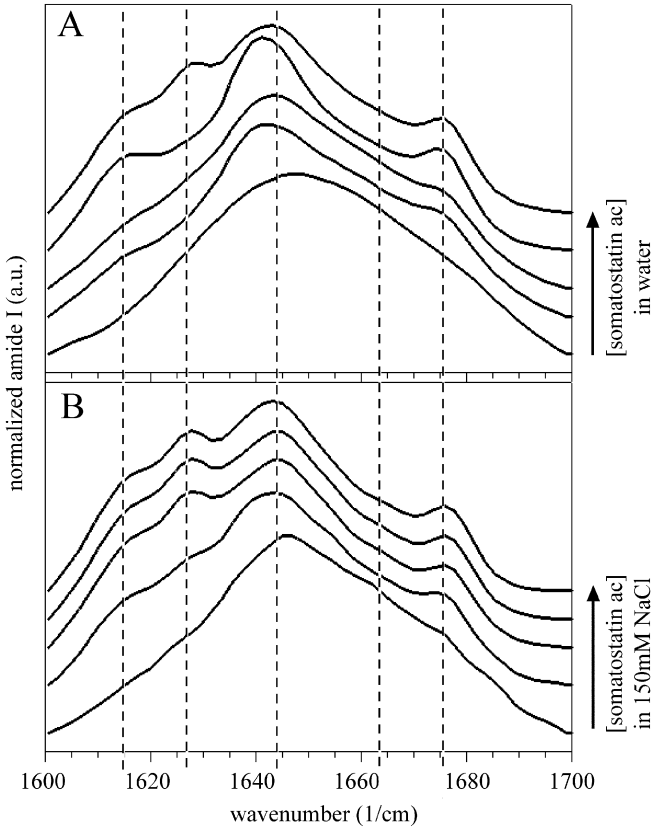

Fig. 7. ATR-FTIR spectra of (A) mesophases of Somatostatin-14 acetate in water as a function of peptide acetate concentration: from down to up, respectively 3%, 5%, 10%, 15% and 20%w/w; and (B) mesophases of Somatostatin-14 acetate in 150 mM NaCl/water as a function of peptide acetate concentration: from down to up, respectively 1%, 3%, 5%, 10% and 15%w/w. Water spectrum was subtracted and baseline corrected. The amide I areas (between 1600 and 1700 cm^{-1}) were normalized.

4. Discussion

Some peptide and protein hormones have been previously reported to self-assemble into β-sheet rich fibrillar supramolecular structures *in vitro*, under disease-related and/or denaturing conditions, in some cases extreme (Haspel et al., 2005; Kajava et al., 2005; Krebs et al., 2004; Reches et al., 2002; Tracz et al., 2004; Waugh, 1946). The results above show that the natural peptide hormone Somatostatin-14 has the intrinsic propensity to self-assemble into supramolecular fibrillar structures, under non-destabilizing and mild solvent conditions. In addition to the implications for general processes of peptide fibrillation, the mild conditions of Somatostatin-14 self-assembly resemble the specific conditions of the regulated hormone secretion pathway, suggesting the hypothesis of biological implications as developed below.

4.1. Structural features of amyloid fibrils

In both pure water and 150 mM NaCl the Somatostatin-14 nanofibrils exhibit structural features previously reported for amyloid fibrils: (i) Congo Red binding, (ii) their morphology and size, i.e., fibrils that are a few microns long and about 7–12 nm wide, (iii) the peptide conformation within the assemblies, i.e., a fixed β-hairpin backbone, from which are developed intermolecular antiparallel β-sheet networks, (iv) the cross-β symmetry of the hydrogen bonds networks relatively to the fibril axis, (v) a structural hierarchy from subfibrillar assemblies, to nanofibrils and to nanofibers *via* lateral twisted associations (Serpell, 2000; Sunde et al., 1997). These features meet the criteria of the definitions currently used for the term amyloid when it only refers to structural types of peptide assemblies (Nilsson, 2004). Additional structural features of the Somatostatin nanofibrils are relevant to other amyloid-like systems without being generic amyloid features. For instance, the tendency for the nanofibril lateral association to occur with a left-handed twist of a regular period could indicate a role for specifically located interactions, although it was only observed in pure water. These could be side-chains interactions, as developed in the model of protofilament interactions for insulin and amylin amyloid fibrils (Jimenez et al., 2002; Kajava et al., 2005). The left-handed sense of twisting has been previously attributed to a structural constraint from the intrinsic left-handed twist between β-strands in β-sheet (Jimenez et al., 2002; Kajava et al., 2005; Salemme and Weatherford, 1981). The presence of four aromatic residues in the Somatostatin-14 sequence suggests that aromatic interactions could be involved in the lateral association. In previous works relevant to our system, such interactions have been proposed to play a significant role, particularly in the cohesion of the liquid crystalline nanotubes formed by the Somatostatin-14 analog Lanreotide, and in the nucleation process and cohesion of characteristic amyloid fibrils (Gazit, 2002; Makin et al., 2005; Valéry et al., 2003, 2004). Our ATR-FTIR data also support the involvement of additional and specific inter-nanofibril interactions in their lateral association into nanofibers, but rather hydrogen bonds networks. Further investigation is therefore needed to elucidate these possible specific interactions responsible for the nanofibrils lateral association.

The Somatostatin-14 self-assembly was found to be sensitive to the addition of NaCl. Relatively to the system in pure water, the presence of 150 mM NaCl was found (i) to favor the self-assembly process, more precisely the limit concentration of liquid crystals formation was found to be about six times lower than in pure water; (ii) to decrease the Somatostatin-14 single nanofibril diameter from 10–11 to 7–8 nm; (iii) to enhance the propensity of nanofibril lateral association. Given that Somatostatin-14 is highly charged (net charge of +2) under the conditions used (pH around 5, calculated p*I* of 8.3), these effects could be explained by the shielding of electrostatic repulsion between the fibrillar objects at each association step, as previously reported for other amyloid-like systems (Chiti et al., 1999; Fujiwara et al., 2003; Zurdo et al., 2001). In the present case, ionic strength is in the right range for which charge shielding not only allows closer lateral association between the objects. It also increases the chances of association and of assuming the correct orientations for optimizing other potential interactions/forces, such as hydrophobic effect and the potential specific interactions discussed above. In this model, the degree of lateral association of the fibrillar objects is dependent on the degree of electrostatic shielding, as observed experimentally.

All the above elements show that the natural peptide hormone Somatostatin-14 is to add to the wide library of natural peptides and proteins able to self-assemble into amyloid fibrils. This finding supports the idea that such a self-association process is a generic feature of polypeptide chains, under appropriate conditions (Chiti et al., 1999; Dobson, 1999). However, the conditions of Somatostatin-14 self-assembly into such architectures are particularly mild when compared to the other natural peptide/protein hormones previously reported to form amyloid fibrils, since Somatostatin is not denatured, self-assembly occurs at room temperature and the solvent conditions are not extreme (water, 150 mM NaCl , pH around 5).

4.2. Non-destabilizing conditions resembling the regulated hormone secretion pathway

Evidence was obtained in favor of the spontaneous self-assembly of Somatostatin-14 into amyloid-like fibrils, under non-destabilizing conditions. First of all, the fixed β-hairpin backbone conformation that Somatostatin-14 adopts within the assemblies was previously established to be directly involved in its bioactivity (Holladay and Puett, 1976; Holladay et al., 1977). The peptide chemical stability within the mesophases, the soft solvent conditions, the fact that the self-assembly process is spontaneous and only involves non-covalent interactions show that the Somatostatin-14 fibrillation is not based on misfolding nor degradation. These features together support that Somatostatin-14 fibrillation is native.

In the presence of 150 mM NaCl, Somatostatin-14 (as acetate salt) was here evidenced to self-assemble into nanofibrils from about 0.5%w/w and at a pH around 5.0. The self-assembly process was observed to occur in a wide range of temperatures, including 37 °C, and the resulting structures were found to be thermodynamically and chemically stable up to much higher temperatures than 37 °C. Although these pH and concentration conditions are not generic physiological conditions, they meet parameters of the specific regulated secretion pathway of peptide/protein hormones, including natural Somatostatin-14 (Burgess and Kelly, 1987). Such peptide/protein hormones are stored into dense-core vesicles, the secretory granules, which are specific storage sites within the secretory cells. Within the secretory granules, peptide/protein hormones are known

to be stored at very high concentrations and at mildly acidic pH (around pH 5.5) (Anderson and Pathak, 1985; Arvan, 1998; Dannies, 1999). Hormones have been further proposed to form "condensed" or "insoluble" aggregates in the regulated secretion pathway, as an element of the sorting mechanisms for the entry in secretory granules, and/or to form high order intermolecular associations for an efficient retention within maturing granules (Arvan, 1998; Chanat and Huttner, 1991). Supporting these hypotheses, newly synthesized insulin from proinsulin was shown to undergo a condensation event, which increases its efficiency of storage in granules (Arvan et al., 1991). Prolactin and growth hormone were shown to be stored as "large insoluble aggregates" in the dense core of secretory granules, and prolactin aggregation was demonstrated to be an important step for the granules formation (Dannies, 2002; Giannattasio et al., 1975; Rambourg et al., 1992). Recent investigations on prolactin further suggested the involvement of self-organized aggregates in these hormone storage mechanisms (Keeler et al., 2004). In addition to pH decrease and hormone concentration, hormone aggregation in the secretory pathway has been proposed to be driven by calcium concentration increase (Arvan, 1998; Dannies, 1999). In the case of Somatostatin-14, the cleavage of the prohormone was reported to occur before the secretory granules formation and the budding of nascent secretory granules was shown not to be calcium mediated (Austin and Shields, 1996; Xu and Shields, 1993).

Somatostatin-14 self-assembly into fibrillar structures that can further undergo lateral packing could therefore be relevant to such an aggregation process involved in the concentration of the natural hormone into nascent secretory granules. This is consistent with concentrating the peptide hormone into dense structures that keep the peptide in its native conformation, since they are built on the peptide bioactive β-hairpin backbone conformation. The fact that Somatostatin-14 is a small and cyclic peptide hormone further restricts its possibilities of conformational behaviors, i.e., likely undergoes self-association *in vivo* as we have characterized it *in vitro*.

Interestingly, Somatostatin-14 immunoreactive amyloid-like aggregates were discovered into multihormone-producing cells of a pancreatic tumor (Takahashi et al., 1998). The amyloid-like morphology reported for these *in vivo* aggregates corresponds to the Somatostatin-14 nanofibrils here obtained *in vitro* under native conditions. In addition, the observation of fibrillar "bundles" and star-like fibrillar arrangements in these cells were reported. These morphologies are also consistent with the spontaneous tendency of the Somatostatin-14 nanofibrils to further associate into higher order nanofibers *in vitro*. The correspondence of these *in vivo* morphologies with our *in vitro* results under native conditions supports that Somatostatin-14 fibrillation could be linked to the secretion and/or oversecretion pathways. The *in vivo* observation of aggregates might have been more likely in such hormone overproducing cells, given the higher concentrations of Somatostatin-14 then expected to occur than in normal secretory cells.

4.3. Functional amyloids?

In addition to the idea that amyloid fibrils are generic features of polypeptide chains under appropriate conditions, the idea that these structures are not necessarily toxic but could be naturally used in non-disease-related functions is emerging today. A growing set of examples, mainly from the bacterial world (Bieler et al., 2005; Chapman et al., 2002; Gebbink et al., 2005) but also including insect (Hamodrakas et al., 2004; Iconomidou et al., 2000), spider (Kenney et al., 2002), and mammalian natural peptides and proteins, supports this concept (Berson et al., 2003). The example of spidroin fibrils making spider silk is particularly relevant to the Somatostatin case (Dicko et al., 2004; Kenney et al., 2002). Spider silks are spun from aqueous solutions. The molecular mechanisms of this process involve the conversion of a highly concentrated, predominantly disordered silk protein (spidroin) into β-sheet rich structures. A liquid crystalline arrangement of spidroin was reported to be established in the storage region in the spider ampulla and to persist in the spider duct, to help store and transport the spidroins in solution, as well as probably control their conversion. Relatively low pH values (around 4) and cations were proposed to make part of the parameters promoting the conversion, i.e., similar environmental parameters as the ones proposed to drive hormone aggregation in secretory cells (Arvan et al., 1991; Dannies, 1999; Dicko et al., 2004). One case of mammalian functional amyloid was reported, that is the fibrillation of the mammalian glycoprotein Pmel17 in the melanosome pathway, to serve as a template for melanin polymerization (Berson et al., 2003; Fowler et al., 2006). This discovery led to the generalized proposition that proteolysis is a way of controlling functional amyloidogenesis in mammalian cells and particularly in lysosome-related organelles. Given that the cleavage of the Somatostatin-14 prohormone was reported to occur in the Golgi apparatus before the secretory granules formation, proteolysis could also be a biological way to control Somatostatin-14 fibrillation (Austin and Shields, 1996; Xu and Shields, 1993).

Next to the above examples of naturally occurring functional amyloid assemblies, our data on Somatostatin-14 fibrillation therefore open the hypothesis of the biological implications of this process, especially the involvement of such mechanisms in the regulated secretion pathway of this natural neuropeptide hormone.

Appendix A. Supplementary data

Supplementary data associated with this article can be found, in the online version, at doi:10.1016/j.jsb.2007.08.006.

References

Anderson, R.G., Pathak, R.K., 1985. Vesicles and cisternea in the trans Golgi apparatus of human fibroblasts are acidic compartments. Cell 40, 635–643.

Arvan, P., 1998. Sorting and storage during secretory granule biogenesis: looking backward and looking forward. Biochem. J. 332, 593–610.

Arvan, P., Kuliawat, R., Prabakaran, D., Zavacki, A.M., Elahi, D., Wang, S., Pilkey, D., 1991. Protein discharge from immature secretory granules displays both regulated and constitutive characteristics. J. Biol. Chem. 266, 14171–14174.

Austin, C.D., Shields, D., 1996. Prosomatostatin processing in permeabilized cells. J. Biol. Chem. 271, 1194–1199.

Berson, J.F., Theos, A.C., Harper, D.C., Tenza, D., Raposo, G., Marks, M.S., 2003. Proprotein convertase cleavage liberates a fibrillogenic fragment of a resident glycoprotein to initiate melanosome biogenesis. J. Cell Biol. 161, 521–533.

Bieler, S., Estrada, L., Lagos, R., Baeza, M., Castilla, J., Soto, C., 2005. Amyloid formation modulates the biological activity of a bacterial protein. J. Biol. Chem. 280, 26880–26885.

Bloom, S.R., Besser, G.M., Roy, V.M., Russell, R.C.G., Schally, A.V., 1974. Inhibition of gastrin and gastric acid secretion by growth hormone release inhibiting hormone. Lancet, 1106–1109.

Bouchard, M., Zurdo, J., Nettleton, E.J., Dobson, C.M., Robinson, C.V., 2000. Formation of insulin amyloid fibrils followed by FTIR simultaneously with CD and electron microscopy. Protein Sci. 9, 1960–1967.

Bouligand ,Y., 1998. Defects and Textures, In: Handbook of Liquid Crystals 1, pp. 406–453.

Brazeau, P., Vale, W., Burgus, R., Ling, N., Butcher, M., Rivier, J., Guillemin, R., 1973. Hypothalamic polypeptide that inhibits the secretion of immunoreactive pituitary growth hormone. Science 179, 77–79.

Burgess, T.L., Kelly, R.B., 1987. Constitutive and regulated secretion of proteins. Annu. Rev. Cell Biol. 3, 243–293.

Chanat, E., Huttner, W.B., 1991. Milieu-induced, selective aggregation of regulated secretory proteins in the trans-Golgi network. J. Cell Biol. 115, 1505–1519.

Chapman, M.R., Robinson, L.S., Pinkner, J.S., Roth, R., Heuser, J., Hammar, M., Normark, S., Hultgren, S.J., 2002. Role of *Escherichia coli* curli operons in directing amyloid fiber formation. Science 295, 851–855.

Chiti, F., Webster, P., Taddei, N., Clark, A., Stefani, M., Ramponi, G., Dobson, C.M., 1999. Designing conditions for in vitro formation of amyloid protofilaments and fibrils. Proc. Natl. Acad. Sci. USA 96, 3590–3594.

Dannies, P.S., 1999. Protein hormone storage in secretory granules: mechanisms for concentration and sorting. Endo. Rev. 20, 3–21.

Dannies, P.S., 2002. Mechanisms for storage of prolactin and growth hormone in secretory granules. Mol. Gen. Metabol. 76, 6–13.

Dicko, C., Kenney, J.M., Knight, D., Vollrath, F., 2004. Transition to a beta-sheet-rich structure in spidroin *in vitro*: the effects of pH and cations. Biochemistry 43, 14080–14087.

Dobson, C.M., 1999. Protein misfolding, evolution and disease. Trends Biochem. Sci. 24, 329–332.

Fowler, D.M., Koulov, A.V., Alory-Jost, C., Marks, M.S., Balch, W.E., Kelly, J.W., 2006. Functional amyloid formation within mammalian tissue. PLoS Biol. 4, e6.

Fujiwara, S., Matsumoto, F., Yonezawa, Y., 2003. Effects of salt concentration on association of the amyloid protofilaments of hen egg white lysozyme studied by time-resolved neutron scattering. J. Mol. Biol. 331, 21–28.

Gazit, E., 2002. A possible role of π-stacking in the self-assembly of amyloid fibrils. FASEB J. 16, 77–83.

Gebbink, M.F.B.G., Claessen, D., Bouma, B., Dijkhuizen, L., Wosten, H.A.B., 2005. Amyloids—a functional coat for microorganisms. Nat. Rev. Microbiol. 3, 333–341.

Giannattasio, G., Zanini, A., Meldolesi, J., 1975. Molecular organization of rat prolactin granules. I. In vitro stability of intact and "membraneless" granules. J. Cell Biol. 64, 246–251.

Goux, W.J., Kopplin, L., Nguyen, A.D., Leak, K., Rytkofsky, M., Shanmuganandam, V.D., Sharma, D., Inouye, H., Kirschner, D.A., 2004. The formation of straight and twisted filaments from short Tau peptides. J. Biol. Chem. 279, 26868–26875.

Guinier, A., 1994. X-ray Diffraction in Crystals Imperfect, Crystals, and Amorphous Bodies. Dover Publication, New York, pp. 219–237.

Hamodrakas, S.J., Hoenger, A., Iconomidou, V.A., 2004. Amyloid fibrillogenesis of silkmoth chorion protein peptide analogues via a liquid crystalline intermediate phase. J. Struct. Biol. 145, 226–235.

Haspel, N., Zanuy, D., Ma, B., Wolfson, H., Nussinov, R., 2005. A comparative study of amyloid fibril formation by residues 15–19 of the human Calcitonin hormone: a single beta-sheet model with a small hydrophobic core. J. Mol. Biol. 345, 1213–1227.

Herrmann, J., Bodmeier, R., 2003. Degradation kinetics of Somatostatin in aqueous solution. Drug Dev. Ind. Pharm. 29, 1027–1033.

Hiramatsu, H., Kitagawa, T., 2005. FT-IR approaches on amyloid fibril structure. Biochim. Biophys. Acta 1753, 100–107.

Holladay, L.A., Puett, D., 1976. Somatostatin conformation: evidence for a stable intramolecular structure from circular dichroism, diffusion, and sedimentation equilibrium. Proc. Natl. Acad. Sci. USA 73, 1199–1202.

Holladay, L.A., Rivier, J., Puett, D., 1977. Conformational studies on somatostatin and analogues. Biochemistry 16, 4895–4900.

Iconomidou, V.A., Vriend, G., Hamodrakas, S.J., 2000. Amyloids protect the silkmoth oocyte and embryo. FEBS Lett. 479, 141–145.

Jimenez, J.L., Nettleton, E.J., Bouchard, M., Robinson, C.V., Dobson, C.M., Saibil, H.R., 2002. The protofilament structure of insulin amyloid fibrils. Proc. Natl. Acad. Sci. USA 99, 9196–9201.

Kajava, A.V., Aebi, U., Steven, A.C., 2005. The parallel superpleated beta-structure as a model for amyloid fibrils of human amylin. J. Mol. Biol. 348, 247–252.

Keeler, C., Hodsdon, M.E., Dannies, P.S., 2004. Is there structural specificity in the reversible protein aggregates that are stored in secretory granules? J. Mol. Neurosci. 22, 43–49.

Kenney, J.M., Knight, D., Wise, M.J., Vollrath, F., 2002. Amyloidogenic nature of spider silk. FEBS J. 269, 4159–4163.

Krebs, M.R.H., MacPhee, C.E., Miller, A.F., Dunlop, I.E., Dobson, C.M., Donald, A.M., 2004. The formation of spherulites by amyloid fibrils of bovine insulin. Proc. Natl. Acad. Sci. USA 101, 14420–14424.

Krimm, S., Bandekar, J., 1986. Vibrational spectroscopy and conformation of peptides polypeptides and proteins. In: Anfinsen, C.B., Edsall, J.T., Richards, F.M. (Eds.), Advances in Protein Chemistry. Academic Press, pp. 181–360.

Nilsson, M.R., 2004. Methods to study amyloid fibril formation in vitro. Methods 34, 151–160.

Makin, O.S., Atkins, E., Sikorski, P., Johansson, J., Serpell, L.C., 2005. Molecular basis for amyloid fibril formation and stability. Proc. Natl. Acad. Sci. USA 102, 315–320.

Mandarino, L., Stenner, D., Blanchard, W., Nissen, S., Gerich, J., 1981. Selective effects of somatostatin-14, -25 and -28 on in vitro insulin and glucagon secretion. Nature 291, 76–77.

Rambourg, A., Clermont, Y., Chretien, M., Olivier, L., 1992. Formation of secretory granules in the Golgi apparatus of prolactin cells in the rat pituitary gland: a stereoscopic study. Anat. Rec. 232, 169–179.

Reches, M., Porat, Y., Gazit, E., 2002. Amyloid fibril formation by pentapeptide and tetrapeptide fragments of human calcitonin. J. Biol. Chem. 277, 35475–35480.

Reisine, T., Bell, G.I., 1995. Molecular biology of somatostatin receptors. Endo. Rev. 16, 427–442.

Salemme, F.R., Weatherford, D.M., 1981. and geometrical properties of β-sheets in proteins. II. Antiparallel and mixed β-sheets. J. Mol. Biol. 146, 119–141.

Schettini, G., 1991. Brain Somatostatin: receptor-coupled transducing mechanisms and role in cognitive functions. Pharmacol. Res. 23, 241–246.

Serpell, L.C., 2000. Alzheimer's amyloid fibrils: structure and assembly. Biochim. Biophys. Acta 1502, 16–30.

Sunde, M., Serpell, L.C., Bartlam, M., Fraser, P.E., Pepys, M.B., Blake, C.C., 1997. Common core structure of amyloid fibrils by synchrotron X-ray diffraction. J. Mol. Biol. 273, 729–739.

Susi, H., Byler, D.M., 1986. Resolution-enhanced Fourier transform infrared spectroscopy of enzymes. Methods Enzymol. 130, 290–311.

Takahashi, M., Hoshii, Y., Kawano, H., Setoguchi, M., Gondo, T., Yamashita, Y., Nakayasu, K., Kamei, T., Ishihara, T., 1998. Multihormone-producing islet cell tumor of the pancreas associated with Somatostatin-immunoreactive amyloid. Am. J. Surg. Path. 22, 360–367.

Tracz, S.M., Abedini, A., Driscoll, M., Raleigh, D.P., 2004. Role of aromatic interactions in amyloid formation by peptides derived from human amylin. Biochemistry 43, 15901–15908.

Valéry, C., Artzner, F., Robert, B., Gulik-Krzywicki, T., Keller, G., Grabielle-Madelmont, C., Torres, M.L., Calvo, P., Cherif-Cheikh, R., Narayanan, T., Paternostre, M., 2004. Self-association process of a peptide in solution: from β-sheet filaments to large embedded nanotubes. Biophys. J. 86, 2484–2501.

Valéry, C., Paternostre, M., Robert, B., Gulik-Krzywicki, T., Narayanan, T., Dedieu, J.C., Keller, G., Torres, M.L., Cherif-Cheikh, R., Calvo, P., Artzner, F., 2003. Biomimetic organization: octapeptide self-assembly into nanotubes of viral capsid-like dimension. Proc. Natl. Acad. Sci. USA 100, 10258–10262.

Valéry, C., Pouget, E., Pandit, A., Boisdé, I., Verbavatz, J.M., Bordes, L., Cherif-Cheikh, R., Artzner, F., Paternostre, M., in press. Molecular origin of the self-assembly of Lanreotide into nanotubes—a mutational approach. Biophys. J.

Veber, D.F., Holly, F.W., Paleveda, W.J., Nutt, R.F., Bergstrand, S.J., Torchiana, M., Glitzer, M.S., Saperstein, R., Hirschmann, R., 1978. Conformationally restricted bicyclic analogs of somatostatin. Proc. Natl. Acad. Sci. USA 75, 2636–2640.

Venyaminov, S.Y., Kalnin, N.N., 1990. Quantitative IR spectrophotometry of peptide compounds in water (H_2O) solutions. I. Spectral parameters of amino acid residue absorption bands. Biopolymers 30, 1243–1257.

Viney, C., Putnam, W.S., 1995. The banded microstructure of sheared liquid-crystalline polymers. Polymer 36, 1731–1741.

Waugh, D.F., 1946. A fibrous modification of insulin. I. The heat precipitate of insulin. J. Am. Chem. Soc. 68, 247–250.

Weckbecker, G., Lewis, I., Albert, R., Schmid, H.A., Hoyer, D., Bruns, C., 2003. Opportunities in somatostatin research: biological, chemical and therapeutic aspects. Nat. Rev. Drug Discov. 2, 999–1017.

Xu, H., Shields, D., 1993. Prohormone processing in the trans-Golgi network: endoproteolytic cleavage of prosomatostatin and formation of nascent secretory vesicles in permeabilized cells. J. Cell Biol. 122, 1169–1184.

Zurdo, J., Guijarro, J.I., Jimenez, J.L., Saibil, H.R., Dobson, C.M., 2001. Dependence on solution conditions of aggregation and amyloid formation by an SH3 domain. J. Mol. Biol. 311, 325–340.